Cancer Research

Androgen Receptor Supports an Anchorage-Independent, Cancer Stem Cell-like Population in Triple-Negative Breast Cancer

Valerie N. Barton[1], Jessica L. Christenson[1], Michael A. Gordon[1], Lisa I. Greene[1], Thomas J. Rogers[1], Kiel Butterfield[1], Beatrice Babbs[1], Nicole S. Spoelstra[1], Nicholas C. D'Amato[1], Anthony Elias[2], and Jennifer K. Richer[1]

Abstract

Preclinical and early clinical trials indicate that up to 50% of triple-negative breast cancers (TNBC) express androgen receptor (AR) and are potentially responsive to antiandrogens. However, the function of AR in TNBC and the mechanisms by which AR-targeted therapy reduces tumor burden are largely unknown. We hypothesized that AR maintains a cancer stem cell (CSC)-like tumor-initiating population and serves as an antiapoptotic factor, facilitating anchorage independence and metastasis. AR levels increased in TNBC cells grown in forced suspension culture compared with those in attached conditions, and cells that expressed AR resisted detachment-induced apoptosis. Culturing TNBC cells in suspension increased the CSC-like population, an effect reversed by AR inhibition. Pretreatment with enzalutamide (Enza) decreased the tumor-initiating capacity of TNBC cells and reduced tumor volume and viability when administered simultaneously or subsequent to the chemotherapeutic paclitaxel; simultaneous treatment more effectively suppressed tumor recurrence. Overall, our findings suggest that AR-targeted therapies may enhance the efficacy of chemotherapy even in TNBCs with low AR expression by targeting a CSC-like cell population with anchorage independence and invasive potential. *Cancer Res; 77(13); 3455–66. ©2017 AACR.*

Introduction

Triple-negative breast cancer (TNBC) is an aggressive breast cancer subtype for which no effective targeted therapies are currently available. Women with TNBC have a peak risk of recurrence between 1 and 3 years, an increased likelihood of distal recurrence, and a higher mortality rate within the first 5 years compared with other breast cancer subtypes (1). Although most metastatic TNBC initially respond to cytotoxic chemotherapy, the majority of patients experience recurrence following treatment (2). Studies suggest that chemotherapy-resistant cancer cells with stem-like properties may repopulate the tumor (3–6). Thus, therapies that target the cancer stem cell (CSC)-like population in combination with chemotherapy may prevent tumor recurrence.

Androgen receptor (AR) protein is expressed to some degree in at least half of all TNBC (7–15), and results of clinical trials targeting AR are promising (14, 16). However, little is known about the function of AR in TNBC and the mechanisms by which AR antagonists improve TNBC outcomes. In ER^+ breast cancer, progesterone and progesterone receptors support the expansion of breast cancer tumor-initiating cells (17), and estrogen and progesterone expand the normal mouse mammary stem cell population, even though it is thought that the stem cells themselves lack estrogen and progesterone receptors (ER and PR; refs. 18, 19). PR and AR recognize similar consensus DNA response elements (20) and regulate many of the same genes (21). In TNBC, AR binds to chromatin at sites more similar to ER in ER^+ breast cancer than AR in prostate cancer (22). Recent studies also suggest that AR may regulate genes associated with CSCs in prostate cancer (23, 24). Finally, we previously reported that the most striking effect of the AR antagonist enzalutamide (Enza) on TNBC was a dramatic decrease in anchorage-independent growth of multiple TNBC cell lines (7).

Based on these data, we hypothesized that in TNBC, in the absence of ER and PR, AR supports a CSC-like population. Identification of AR as a target that maintains a tumor-initiating population may alter the clinical treatment strategy. AR antagonists may, in fact, not only target AR^+ tumor cells, but also a chemotherapy-resistant CSC population. Our research demonstrates that AR is increased in TNBC under anchorage-independent conditions, and AR inhibition decreases CSC-like populations *in vitro* and tumor initiation *in vivo*. Finally, Enza enhances the efficacy of chemotherapy in a preclinical model and reduces recurrence when given simultaneously with chemotherapy.

Materials and Methods

Cell culture

All cell lines were authenticated in 2014 by Short Tandem Repeat DNA Profiling (Promega) at the University of Colorado Cancer Center (UCCC) Tissue Culture Core, and testing for

[1]Department of Pathology, University of Colorado Anschutz Medical Campus Aurora, Colorado. [2]Department of Medicine University of Colorado Anschutz Medical Campus, Aurora, Colorado.

Note: Supplementary data for this article are available at Cancer Research Online (http://cancerres.aacrjournals.org/).

V.N. Barton and J.L. Christenson contributed equally to this article.

Corresponding Author: Jennifer K. Richer, Department of Pathology, University of Colorado Anschutz Medical Campus, 12800 E 19th Avenue, Aurora, CO 80045. Phone: 303-724-3711; Fax: 303 724-3712; E-mail: jennifer.richer@ucdenver.edu

doi: 10.1158/0008-5472.CAN-16-3240

mycoplasma was performed every 3 months. Only cells under five passages were used in this study. SUM159PT cells were purchased from the UCCC Tissue Culture Core in 2013 and were grown in Ham's F-12 with 5% fetal bovine serum (FBS), penicillin/streptomycin (P/S), hydrocortisone, insulin, HEPES, and L-glutamine supplementation. BT549 cells, purchased from the ATCC in 2008, were grown in RPMI Medium 1640 with 10% FBS, P/S and insulin. MDA-MB-453 (MDA453) cells, purchased from ATCC in 2012, were grown in DMEM Medium with 10% FBS and P/S.

SUM159PT-TGL cells were generated by stable retroviral transduction with a SFG-NES-TGL vector, encoding a triple fusion of thymidine kinase, green fluorescent protein and luciferase, and sorted for green fluorescent protein. SUM159PT and MDA453 AR knockdown cells were generated by lentiviral transduction of shRNAs-targeting AR (pMISSION VSV-G, Sigma Aldrich), including AR shRNA 3715 (shAR15) and AR shRNA 3717 (shAR17). Lentiviral transduction of pMISSION shRNA NEG (shNEG) was used as a nontargeting control. Plasmids were purchased from the University of Colorado Functional Genomics Core Facility.

Cellular assays and reagents

Cells were treated with 20 μmol/L Enza (Medivation) and 10 nmol/L dihydrotestosterone (DHT, Sigma Aldrich). Twenty μmol/L Enza approximates the IC_{50} of the cell lines studied and is a clinically achievable concentration. Circulating plasma C_{max} values for Enza and its active metabolite (*N*-desmethyl enzalutamide) are 16.6 μg/mL (23% CV) and 12.7 μg/mL (30% CV), respectively (Enza package insert Exposure Rationale), which is equivalent to approximately 60 μmol/L total active drug in plasma at steady state.

Forced suspension culture

Poly-2-hydroxyethyl methacrylate (poly-HEMA, Sigma) was reconstituted in 95% ethanol to 12 mg/mL. Culture plates were coated with poly-HEMA and incubated overnight to allow ethanol evaporation. Plates were washed with phosphate-buffered saline (PBS) prior to use.

Gene expression array analysis

BT549 cells were grown in either attached or forced suspension condition in quadruplicate for 24 hours. RNA was harvested using the TRIzol method and hybridized onto Affymetrix Human Gene 1.0ST arrays at the University of Colorado Denver Genomics and Microarray Core, following the manufacturer's instructions. The array data are available in the Gene Expression Omnibus (GEO) database as GSE95472.

Microarray analysis was performed using Partek Genomics Suite (Partek, Inc.) and MetaCore Pathway Analysis software (Thomson Reuters). One-way ANOVA analysis was performed to determine differentially expressed genes between the two treatment groups. Significantly differentially expressed genes were imported to MetaCore for pathway analysis, including identification of altered canonical pathways. Determination of potentially AR-regulated genes was performed by gene searches on the Androgen Responsive Gene Database (http://software.broadinstitute.org/gsea/msigdb/).

Quantitative RT-PCR

RNA was isolated by TRIzol (Invitrogen) and cDNA was synthesized from 1 μg total RNA, using M-Mulv reverse transcriptase enzyme (Promega). SYBR Green quantitative gene expression analysis was performed using the following primers: *AR* forward, 5′-CTCACCAAGCTCCTGGACTC-3′ and *AR* reverse, 5′-CAGGCAGAAGACATCTGAAAG-3′; *GR* forward, 5′-ACTGCCCCAAGTGAAAACAGA-3′ and *GR* reverse, 5′-ATGAACAGAAATGGCAGACATTT-3′; *β-ACTIN* forward, 5′-CTGTCCACCTTCCAGCAGATG-3′ and *β-ACTIN* reverse, 5′-CGCAACTAAGTCATAGTCCGC-3′; and *RPL13A* forward, 5′-CCTGGAGGAGAAGAGGAAAGAGA-3′ and *RPL13A* reverse, 5′-TTGAGGACCTCTGTGTATTTGTCAA-3′. Relative gene expression was calculated using the comparative cycle threshold method and values were normalized to *β-ACTIN* or *RPL13A*.

Immunoblotting

Whole-cell protein extracts (50 μg) were denatured, separated on SDS-PAGE gels and transferred to polyvinylidene fluoride membranes. After blocking in 3% bovine serum albumin in Tris-buffered saline–Tween, membranes were probed overnight at 4°C. Primary antibodies include AR (PG-21, 1:500 dilution; EMD Millipore), GR (1:1000 dilution; Cell Signaling Technology), and α-tubulin (clone B-5-1-2, 1:30,000 dilution; Sigma Aldrich). Following secondary antibody incubation, results were detected using Western Lightning Chemiluminescence Reagent Plus (Perkin Elmer).

Immunocytochemistry and Immunofluorescence

Cells were plated in poly-HEMA coated or uncoated plates for 24–96 hours, fixed in 10% neutral buffered formalin, pelleted in histogel (Thermo Fisher), and paraffin embedded by the UC Denver Tissue Biobanking and Processing Core. Slides were deparaffinized in a series of xylenes and ethanols, and antigens were heat retrieved in either 10 mmol/L citrate buffer pH 6.0 or 10 mmol/L Tris/1 mmol/L EDTA pH 9.0. Antibodies used were AR clone 441 (Dakocytomation) or AR clone SP107 (Cell Marque). The Vectastain Elite ABC Kit (Vector Laboratories Inc.) or Envision horseradish peroxidase (Dakocytomation) were used for detection, and Tris-buffered saline with 0.05% Tween 20 was used for all washes. Representative images were taken using a BX40 microscope (Olympus) with a SPOT Insight Mosaic 4.2 camera and software (Diagnostic Instruments, Inc.).

For Immunofluorescence, antibodies to cleaved-caspase-3 (Cell Signaling Technology) and AR (clone SP107) were used in duplex with TSA Plus Cyanine 3.5 and Fluorescein kits, respectively per manufacturer's instructions (Perkin Elmer). Images were taken using a BX40 microscope, DP73 camera, and cellSens standard software (Olympus). In addition, slides were scanned using a Vectra 3 quantitative pathology imaging system and inForm 2.2 software was used to obtain a percent positive score for cells in $n = 3$ fields after both cell segmentation and phenotype analysis (Perkin Elmer).

CSC-like population analysis

For the mammosphere formation assays, single cells were plated in 96-well ultra-low attachment plates in 200 μL per well of Mammocult media (Stem Cell Technologies). After incubating for 1 week, the number of mammospheres present was determined by microscopy. Mammosphere criteria included at least five cells and a length of at least 50 μm. The mammosphere formation efficiency (MFE) was calculated as the number of mammospheres formed divided by the number of single

cells plated. CD44/CD24 (BD Biosciences) staining was conducted per the manufacturer's protocol by flow cytometry analysis. The ALDEFLUOR assay (Stem Cell Technologies) was performed per the manufacturer's protocol. ALDEFLUOR-positive and -negative cell populations were sorted with the assistance of the University of Colorado Cancer Center Flow Cytometry Shared Resource on the MoFlo XDP100 cell sorter (Beckman Coulter Life Sciences).

Tumor studies

Xenograft experiments were approved by the University of Colorado Institutional Animal Care and Use Committee [IACUC protocol 83614(01)1E] and conducted in accordance with the National Institutes of Health Guidelines for the Care and Use of Laboratory Animals. For the limiting dilution study, a range of 10^2–10^6 SUM159PT-TGL cells were mixed with Matrigel (BD Biosciences) and bilaterally injected into the mammary fat pads of five female, athymic nu/nu mice (Taconic). Cells were treated before injection with 20 μmol/L Enza or vehicle control (1% DMSO) for 72 hours. Tumor burden was assessed by luciferase activity and by caliper measurements (tumor volume was calculated as volume = (length × width^2)/2). Mice were euthanized by carbon dioxide asphyxiation followed by cervical dislocation, and the tumors were harvested.

For the Enza and paclitaxel (Pac) study, 10^6 SUM159PT-TGL cells were mixed with Matrigel (BD Biosciences) and bilaterally injected into the mammary fat pads of female, athymic nu/nu mice (Taconic). Tumor burden was assessed by luciferase activity and by caliper measurements. Once tumors were established, mice were matched into groups based on the total tumor burden as assessed by luciferase activity and by caliper measurements. Mice were administered Enza in their chow (approximately 50 mg/kg daily dose). Enza was mixed with ground mouse chow (Research Diets Inc.) at 0.43 mg/g chow. The feed was irradiated and stored at 4°C before use. Mice in the control group received the same ground mouse chow but without Enza. Mice were given free access to either Enza formulated chow or control chow throughout the study period. Mice were given Pac (LTK Labs) intraperitoneally at a dose of 10 mg/kg/d for 5 consecutive days. Stock Pac was prepared in 50% ethanol and 50% Kolliphor EL (Sigma), then diluted in PBS to a concentration of 1 mg/mL. Mice were euthanized by carbon dioxide asphyxiation followed by cervical dislocation and tumors were harvested.

Statistical significance

Statistical significance was evaluated using a two-tailed Student *t* test or ANOVA with GraphPad Prism software. Binomial probability was used to calculate significance of MFE assays. Extreme limiting dilution analysis (ELDA) was used to calculate stem cell frequency and significance of tumor initiation frequency of the limiting dilution assay. A P value of less than 0.05 was considered statistically significant.

Results

AR transcript, protein, and transcriptional activity are upregulated in forced suspension culture compared with adherent conditions

To determine what genes may have a role in the ability of cells to resist anoikis and survive in suspension (mimicking survival in-transit during metastasis), gene expression microarray analysis was conducted on BT549 cells following growth in attached or forced suspension culture for 24 hours (GEO record GSE95472). Data analysis was performed to identify genes significantly altered by more than 2.0-fold between attached and suspended conditions by one-way ANOVA analysis ($P < 0.05$). Among the 73 genes differentially expressed >2.0-fold, 30 were potentially AR-regulated, as determined by cross-referencing with the Androgen Responsive Gene Database (http://software.broadinstitute.org/gsea/msigdb/; Fig. 1A). Metacore pathway analysis revealed that AR was one of the top predicted upstream regulators of genes altered in BT549 cells cultured in suspension (Fig. 1B).

Upon further investigation, we found that *AR* transcript was significantly increased after 24 hours in forced suspension compared with the attached condition in three TNBC cell lines (MDA453, SUM159PT, and BT549; Fig. 2A). As many TNBC cell lines also express the glucocorticoid receptor (GR), we examined *GR* transcript levels and found that they were unchanged between cells in suspension and attached culture (Fig. 2A). Increased AR, but not GR protein was detected in cells in forced suspension culture by Western blot after 48 hours (Fig. 2B). The increase in AR protein was confirmed by IHC after 48 hours in attached versus forced suspension culture followed by paraffin embedding (Fig. 2C). Although the Western and IHC both demonstrated much lower baseline levels of AR in the BT549 and SUM159PT cells as well as fewer AR^+ cells compared with MDA453, IHC revealed that AR clearly increases in a small percentage of cells in the BT549 and SUM159PT. Interestingly, the latter two cell lines aggregated in suspension culture and there was at least one AR^+ cell per clump. Indeed, with increased time in suspension culture, the BT549 cells showed enrichment for both the percent AR^+ cells and AR-staining intensity compared with attached culture conditions (Supplementary Fig. S1). AR transcriptional activity on a consensus AR response element (ARE) linked to luciferase was significantly increased in suspended compared with attached conditions in SUM159PT and BT549 cells. This effect was attenuated in cells transduced with shRNAs targeting AR (Fig. 2D).

AR^+ cells are resistant to apoptosis

We previously reported that Enza caused a greater than 80% reduction in TNBC cell growth on soft agar (7). As AR expression and activity were increased in forced suspension culture, we hypothesized that AR might protect against anoikis (detachment-induced cell death). Dual immunofluorescent staining of AR and the active apoptotic marker cleaved-caspase-3 (CC3) demonstrated increased staining in MDA453 and BT549 cells following 48 hours in forced suspension culture (Fig. 3A). The MDA453 cells, that are highly AR^+, showed less CC3 staining than the BT549. Importantly, these two markers were found to be mutually exclusive (Fig. 3B), with less than 1% of cells costaining for both AR and CC3 (Fig. 3C). In other words, AR^+ cells did not undergo apoptosis in suspension culture.

A population of CSC-like cells increases in forced suspension conditions

Anchorage independence is associated with stem cells and we, therefore, expected the CSC-like population to be increased in forced suspension culture conditions. $CD44^+/CD24^-$ staining was used to identify CSC-like MDA453 cells. Although there

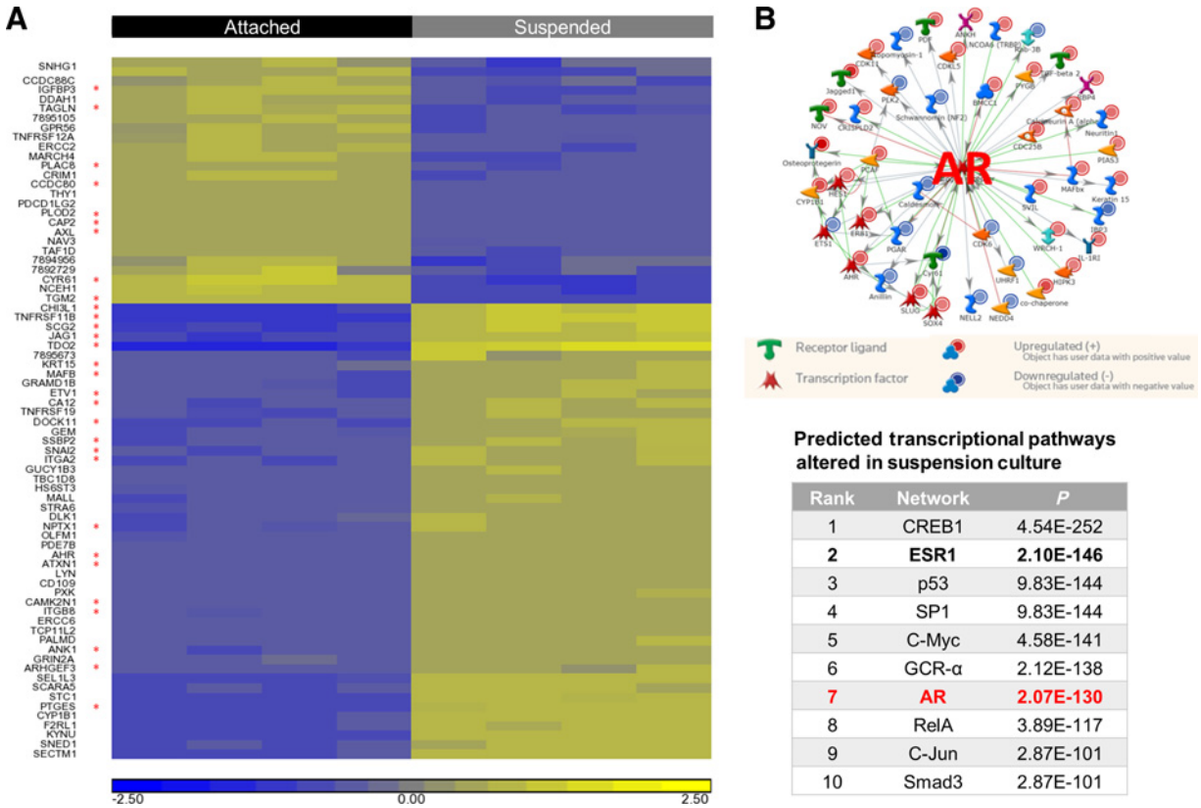

Predicted transcriptional pathways altered in suspension culture

Rank	Network	*P*
1	CREB1	4.54E-252
2	**ESR1**	**2.10E-146**
3	p53	9.83E-144
4	SP1	9.83E-144
5	C-Myc	4.58E-141
6	GCR-α	2.12E-138
7	**AR**	**2.07E-130**
8	RelA	3.89E-117
9	C-Jun	2.87E-101
10	Smad3	2.87E-101

Figure 1.

AR-regulated changes in gene expression in TNBC cells cultured in forced suspension. **A,** Heatmap of genes differentially regulated in BT549 cells grown in attached versus suspended culture conditions for 24 hours. Biological quadruplicate samples of each treatment group are shown. Genes with > or < 2.0 fold-change difference between attached and suspended conditions ($P < 0.05$) are shown (yellow, increased gene expression; blue, decreased gene expression). Red stars, potentially AR-regulated genes in the Androgen Responsive Gene Database (http://software.broadinstitute.org/gsea/msigdb/). **B,** MetaCore analysis of BT549 microarray data. Top, pathway analysis illustrating annotated connections between AR and genes altered in suspension culture. Bottom, summary of top transcriptional pathways predicted to be altered in suspension compared with attached culture conditions.

were no changes in CD44 staining (data not shown), CD24 staining decreased by 2-fold following suspension culture, suggesting a less luminal phenotype (Fig. 4A, $P < 0.001$). A 2-fold increase in MFE was also observed in MDA453 cells placed in suspension culture for 5 days prior to plating the mammosphere assay (Fig. 4B, $P < 0.05$). These findings were confirmed in a second cell line, SUM159PT, where a 3-day forced suspension culture of SUM159PT cells increased the population of aldehyde dehydrogenase-positive ($ALDH^+$) cells to 60%, compared with 40% in attached culture (Fig. 4C, $P < 0.01$). Likewise, in a MFE assay, SUM159PT cells suspended 3 days prior to initiation of the assay exhibited a 5-fold increase in MFE (Fig. 4D, $P < 0.001$). An examination of AR gene expression in the $ALDH^+$ versus ALDH- populations of SUM159PT cells cultured in forced suspension, showed that $ALDH^+$ SUM159PT cells expressed significantly higher AR mRNA levels than the ALDH- population, suggesting that the CSC-like SUM159PT cell population is AR^+ (Fig. 4E, $P < 0.0001$).

AR inhibition decreases the CSC-like population *in vitro*

Because we observed that the increase in *AR* expression and activity coincided with an enrichment of CSC-like cells in suspension culture, we next tested whether inhibiting AR could decrease the CSC-like population. In SUM159PT cells, AR knockdown decreased the percentage of $ALDH^+$ cells from 55% to approximately 40% (Fig. 5A, $P < 0.001$). A 4-fold decrease in MFE was also observed (Fig. 5B, $P < 0.05$) following AR knockdown. Finally, treatment with the AR antagonist Enza decreased MFE by nearly 2-fold (Fig. 5C, $P < 0.01$). These results were recapitulated in the MDA453 cell line. AR knockdown led to a decrease in the $CD44^+/CD24^-$ cell population, as shown by an increase in the levels of CD24 following knockdown, indicative of a more luminal phenotype (Fig. 5D, $P < 0.05$). Similarly, AR knockdown decreased MFE in MDA453 by 2-fold (Fig. 5E, $P < 0.05$). Treatment with Enza decreased MFE in MDA453 (Fig. 5F, $P < 0.001$), and although a trend toward decreased mammosphere length was observed following AR inhibition, these changes did not reach statistical significance.

Pretreatment with enzalutamide decreases tumor initiation frequency *in vivo*

To evaluate the effect of AR inhibition on the CSC property of tumor initiation, an *in vivo* limiting dilution assay was performed. Luciferase-tagged SUM159PT cells were pretreated for

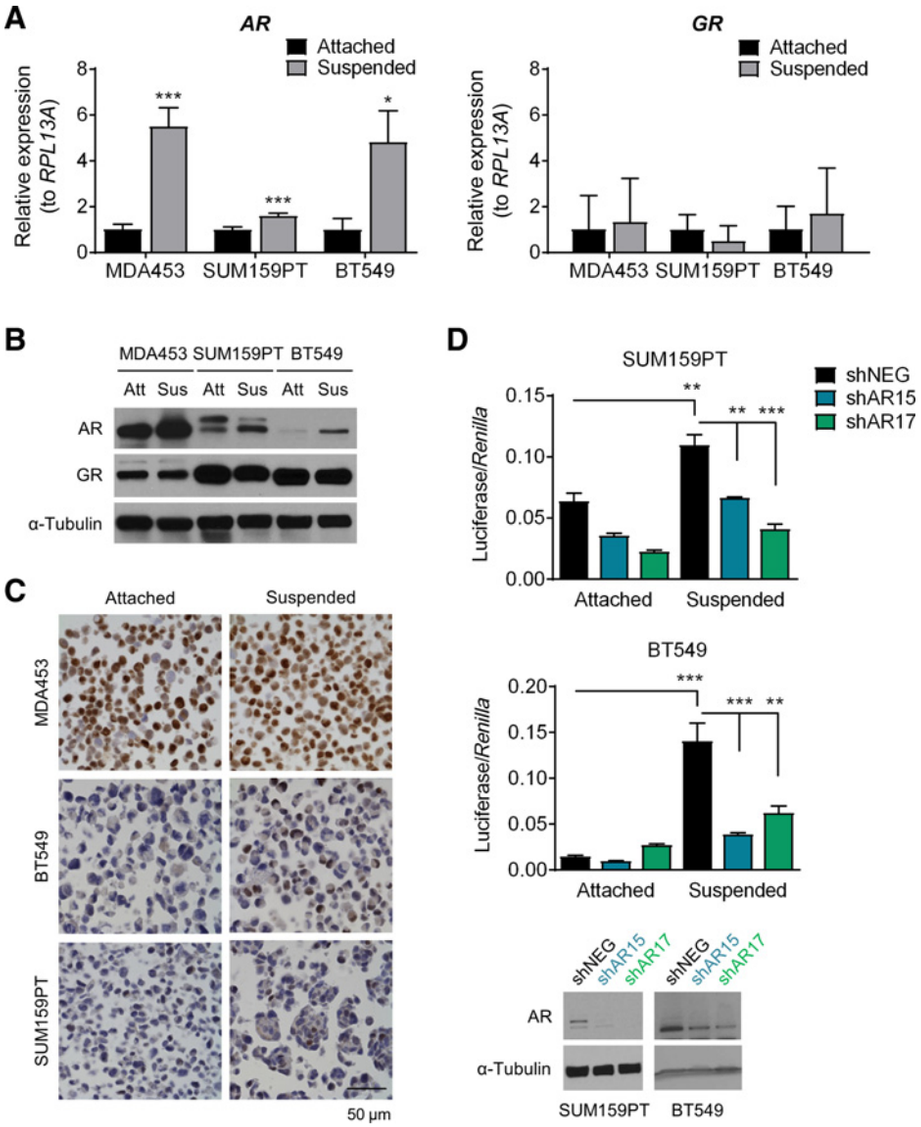

Figure 2.
AR expression increases in forced suspension culture. **A,** qRT-PCR for *AR* and *GR* gene expression in attached versus forced suspension culture conditions at 24 hours. **B,** Western blot for AR and GR in attached versus forced suspension culture conditions at 24 hours. α-Tubulin was used as a loading control. **C,** Immunohistochemistry for AR in attached versus forced suspension culture conditions at 48 hours. Representative images, magnification, ×400. **D,** AR luciferase reporter assay in attached compared with suspended conditions in cells transduced with a nontargeting control (shNEG) or shRNAs targeting AR (shAR15, shAR17). Western blot for AR. α-Tubulin was used as a loading control. Mean ± SD; *, $P < 0.05$; **, $P < 0.01$; ***, $P < 0.001$.

3 days with either vehicle or Enza *in vitro*. Mice received bilateral orthotopic injections in the fourth mammary gland of these cells ranging from 10^2–10^6 cells and tumor formation was measured by palpation and luciferase activity (Fig. 6A and B, Supplementary Fig. S2). By both analyses, pretreatment with Enza significantly decreased the tumor-initiation frequency by approximately 2.5-fold (Fig. 6B bottom, $P < 0.05$), suggesting that inhibition of AR decreases the tumor-forming ability of TNBC cells.

Combined enzalutamide plus paclitaxel is more effective than paclitaxel alone

CSCs are resistant to chemotherapy and may repopulate the tumor following treatment (3–6). Given that AR inhibition decreases the CSC-like population *in vitro* and *in vivo* (Figs. 5 and 6), AR inhibition combined with chemotherapy may prove to be more effective than chemotherapy alone. *In vitro*, both Enza and Pac inhibit SUM159PT cell growth more than 50% ($P < 0.001$). However, the combination of drugs inhibited cell growth by 75% (Supplementary Fig. S3A, $P < 0.01$).

To determine *in vivo* whether the combination of AR inhibition and chemotherapy is more effective than chemotherapy alone, Enza was administered to mice either simultaneously (SIM) or subsequent (SEQ) to Pac and these mice were compared with mice-administered Pac alone (see Supplementary Fig. S3B for experimental design and Supplementary Fig. S3C for matched group randomization). Tumor viability analysis demonstrated that the addition of Enza (whether SIM or SEQ) significantly decreased tumor viability compared with Pac alone (Fig. 7A and B). Tumor volume was also significantly smaller in both groups that received Pac plus Enza compared with Pac alone ($P < 0.05$; Fig. 7C and D). Only mice treated SIM with Enza and Pac showed a statistically significant reduction in tumor viability (Fig. 7E), indicating that only this group did not exhibit recurrance. These findings suggest that giving Enza in combination with chemotherapy may effectively

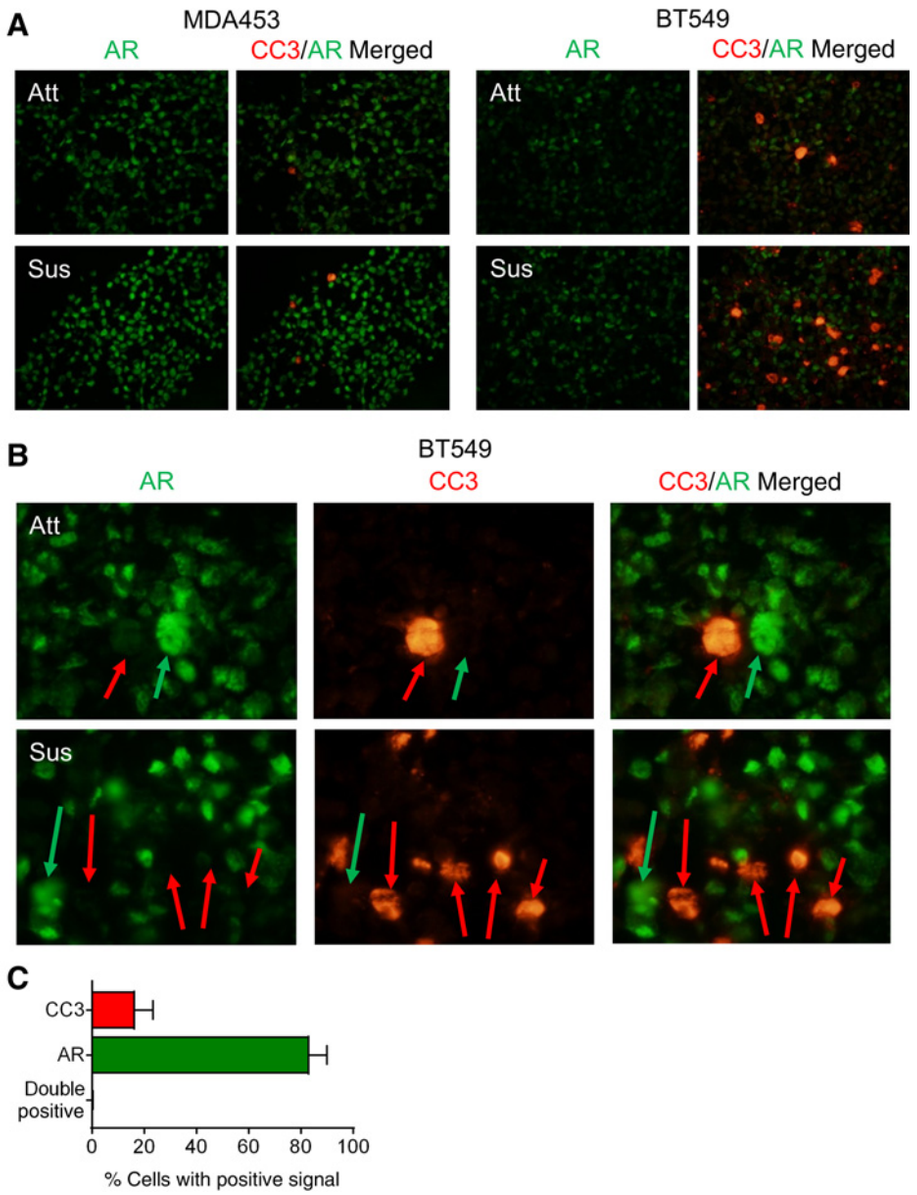

Figure 3.
AR and cleaved-caspase-3 (CC3) increase in TNBC cells cultured in forced suspension and do not colocalize. **A** and **B,** TNBC cells were grown in attached and suspended conditions for 48 hours and stained for AR (green) and CC3 (red) using tyramide signal amplification. Representative images, magnification, ×400 (**A**) and magnification ×1,000 (**B**), to emphasize CC3 (red arrows) and AR (green arrows) localization. **C,** Image analysis of BT549 suspended cells using inForm 2.2. Percentage of cells positive for Cy3.5 (CC3), FITC (AR), or double positive ($CC3^+AR$) were calculated from the total number of positive cells for $n = 3$ random 200× fields; mean ± SEM.

reduce recurrance following cessation of chemotherapy treatment.

Discussion

Our data demonstrate the novel finding that AR mRNA, protein, and transcriptional activity are upregulated in TNBC cell lines under anchorage-independent conditions. We previously published that the antiandrogen Enza dramatically reduced growth on soft agar, a classic measure of anchorage independence, in multiple TNBC cell lines (7). The data presented here indicate that AR is increased in forced suspension culture and protects against cell death under anchorage-independent conditions. This data is consistent with previous studies demonstrating that AR^+ tumors retain AR expression in metastatic disease (25, 26). Interestingly, Lawson and colleagues recently reported single-cell sequencing of circulating tumor cells from TNBC patient-derived xenografts (PDX) and found *AR* among the transcripts upregulated in circulating tumor cells (CTC) and low-burden metastases compared with the primary tumor (21.5 fold; ref. 27); however, they did not examine AR protein. Taken together, these data suggest that AR may support survival in transit during metastasis.

The present data also demonstrate, both *in vitro* and *in vivo*, that AR inhibition decreases a CSC-like population. A recent article by Feng and colleagues reports an increase in cancer cell stemness and invasive potential following increased AR expression and activation in ER^+ MCF7 breast cancer cells (28). Furthermore, AR is highly retained in lung metastases in the MMTV-PyMT mammary carcinoma model that arise from tumors that are intially ER^+/PR^+, but loose ER and PR prior to metastasis (29). Our finding that AR inhibition affects

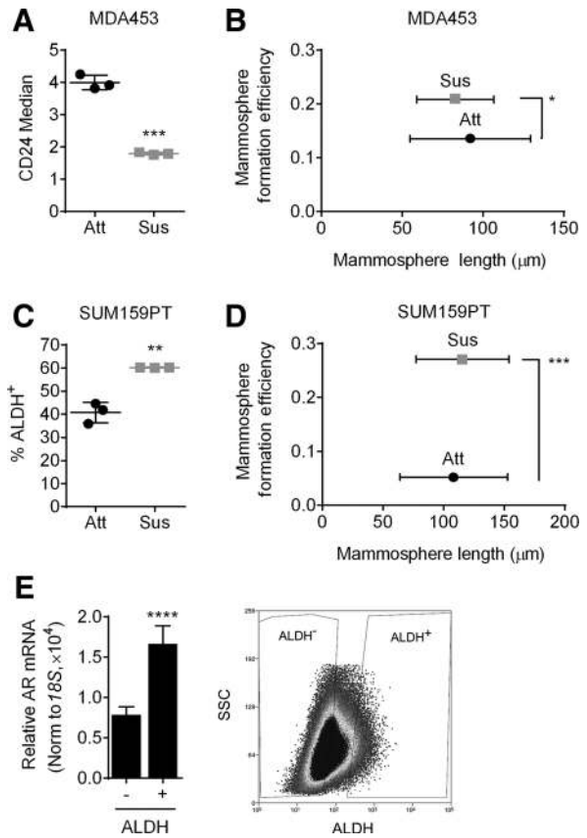

Figure 4.

A CSC-like population is increased in suspension. **A,** CD24 staining of MDA453 cells following 5 days in suspension culture. **B,** MFE assay of MDA453 cells placed in attached or suspended conditions for 5 days prior to plating. **C,** ALDEFLUOR ($ALDH^+$) assay of SUM159PT cells placed in suspended conditions for 3 days. DEAB was used as a control to set the gate. **D,** MFE assay of SUM159PT cells placed in attached or suspended conditions for 3 days prior to plating. **E,** SUM159PT cells cultured for 3 days in suspension were sorted for ALDH and *AR* gene expression was measured using qRT-PCR. Shown is a representative image of sorted ALDH populations. Mean ± SD; *, $P < 0.05$; **, $P < 0.01$; ***, $P < 0.001$; ****, $P < 0.0001$.

a CSC-like population challenges the theory that AR-targeted therapies will only be effective in tumors with high AR (30–32), because even if AR is only expressed in a small number of cells it can still influnce whether latent CSC-like cells persist after therapy and cause recurrant disease. Indeed, preliminary data from the phase II trial of Enza in TNBC demonstrated that the degree of AR immunostaining itself was not the best predictor of who will receive the most benefit from AR-targeted therapy, but rather a signature of genes indicative of AR activity (16). If AR-targeted therapies decrease the CSC-like population capable of repopulating a tumor to form local or distant recurrence, then even patients with relatively low AR expression may benefit from antiandrogens because these cells represent a slow growing CSC-like population that can survive chemotherapy. This finding is not unprecidented as breast cancer patients with as low as 1% ER positivity in their primary tumors can benefit from ER-targeted therapies, although a definative mechanism for this phenomenon has not, to date, been elucidated.

Estrogen and progesterone expand the stem cell population in the normal mammary gland and breast cancer (18, 19). In AR^+ TNBC, AR binds to many of the same sites on chromatin as ER binds in ER^+ breast cancer (22). In mammary epithelial cells amphiregulin (AREG), transcriptionally regulated by ER, supports the expansion of stem cells (18, 19, 33). Our previously published data demonstrated that activation of AR in TNBC cell lines increased AREG production *in vitro* and *in vivo* and treatment with Enza significantly abbrogated AREG (7). In the present study, we identified genes altered by 24 hours in forced suspension culture in the TNBC line BT549 (Fig. 1A). Interestingly, many of the top genes that increase in suspension culture are known to be AR-regulated and encode factors such as jagged-1 (JAG1, a ligand for Notch receptors and target of the canonical WNT-signaling pathway in progenitor cells) and chitinase (CHI3L1 or YKL40, which is well known to be androgen-regulated in prostate cancer). TNFRSF11B or osteoprotegerin, the receptor for RANKL/osteoprotegerin ligand (TNFSF11), was also increased in suspension culture and is AR regulated. Any and all of these AR-regulated proteins may mediate survival of an anchorage-independent, stem-like population. AR^+ cells may support a CSC-like population through such paracrine action or may themselves have stem-like properties, as indicated by this study. Although there is a very low percentage of $CD44^+$ cells in the luminal AR MDA453 line, as reported previously (34), and this does not change with suspension culture (data not shown), CD24 staining decreased by 2-fold following suspension culture, perhaps suggesting a slightly less luminal or more flexible phenotype (Fig. 4A). The percentage of cells positive for AR at baseline in the MDA453 is high, but still increased in suspension (Figs. 2B and C and 3A). AR confers a luminal gene expression pattern by binding to chromatin at sites where ER binds in ER^+ breast cancer lines (22). Indeed, we observe that the majority of MDA453 cells do not die in forced suspension (Fig. 3A), indicating that there are cells that are luminal, but resistant to anoikis (a trait usually associated with mesenchymal/CSCs). When AR was knocked down, the $CD24^+$ population increased (Fig. 5D) and mammosphere formation efficiency decreased with the antiandrogen enzalutamide (Fig. 5F), indicating that AR affects these CSC-like traits. Although further studies are needed to elucidate the mechanisms by which AR supports a CSC-like population or whether the AR^+ cells themselves are the CSC-like tumor initiating population, we find AR transcript to be more abundant in the $ALDH^+$ population of SUM159PT cells. Collectively these data demonstrate that AR inhibition decreases mammosphere formation efficiency *in vitro* and tumor initiation *in vivo*.

Given the success of Enza (Xtandi) in metastatic TNBC (NCT01889238; ref. 16), the next trials will test efficacy of antiandrogens in combination with chemotherapy as frontline therapy and in the neoadjuvant setting. The need for improved chemotherapy among AR^+ TNBC tumors is highlighted in a study by Masuda and colleagues demonstrating that AR^+ TNBCs (luminal AR subtype) have a poor pathologic complete response compared with other subtypes (35). This is likely because AR^+ tumors proliferate more slowly and are, therefore, less responsive to chemotherapeutic agents. Antiandrogens may increase the efficacy of chemotherapy by decreasing the CSC population that is insensitive to chemotherapy and repopulates the tumor

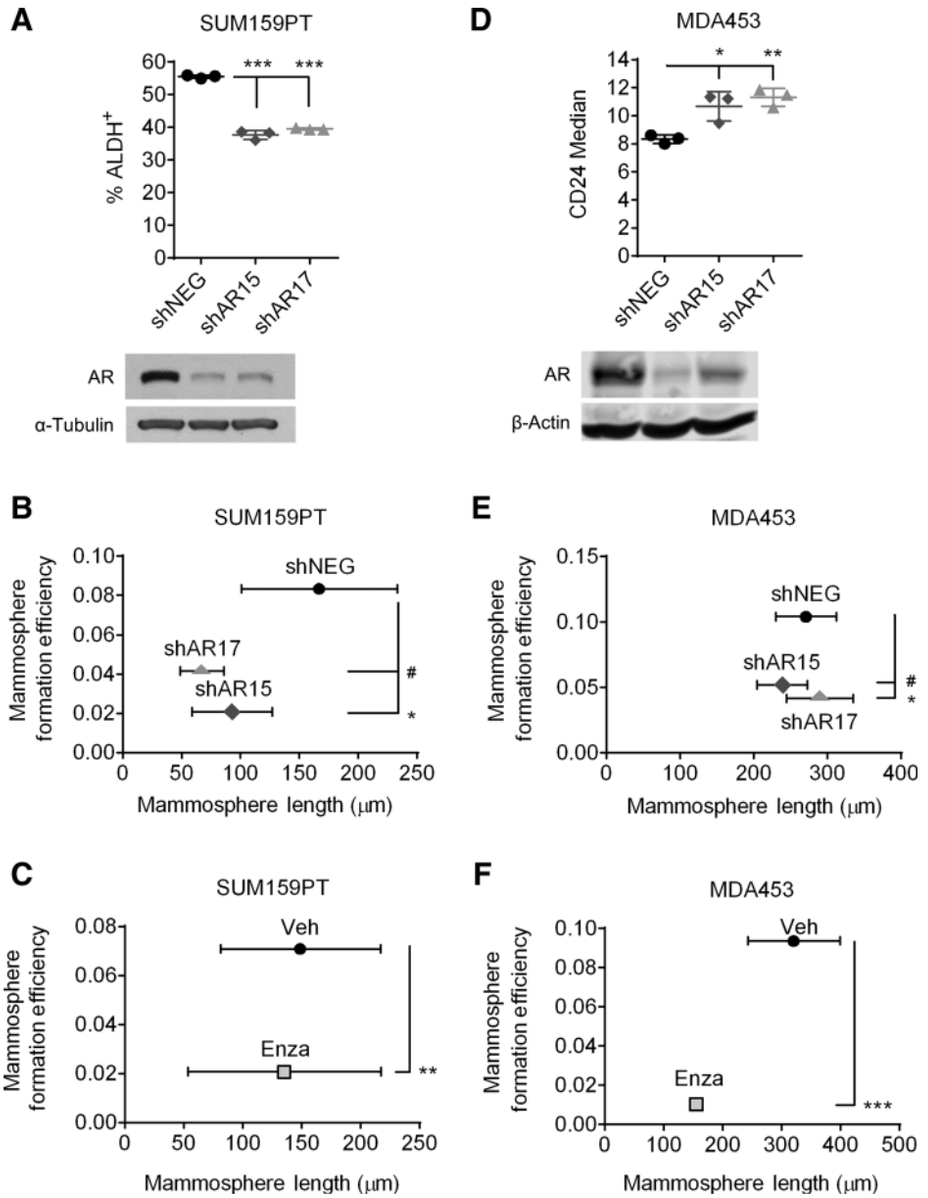

Figure 5.
AR inhibition decreases a CSC-like population. **A,** ALDEFLUOR assay of SUM159PT cells transduced with a nontargeting control (shNEG) or shRNAs targeting AR (shAR15 and shAR17). Western blot for AR. α-Tubulin is shown as a loading control. **B** and **C**, MFE assays of SUM159PT cells transduced with shNEG, shAR15, or shAR17 (**B**) or treated with Enza (**C**). **D,** CD24 staining of MDA453 cells transduced with shNEG, shAR15, or shAR17. Western blot for AR. β-Actin is shown as a loading control. **E** and **F,** MFE assays of MDA453 cells transduced with shNEG, shAR15, or shAR17 (**E**) or treated with Enza (**F**). Mean ± SD; *, $P < 0.05$; #, $P = 0.06$; **, $P < 0.01$; ***, $P < 0.001$.

postchemotherapy to cause relapse (3–6). This study indicates that the combination of Enza and chemotherapy is more effective than chemotherapy alone in a preclinical model. Although both Enza plus chemotherapy regimens (simultaneous and subsequent) were more effective than chemotherapy alone, simultaneous treatment yielded significantly decreased tumor volume and viability and no regrowth upon cessation of chemotherapy.

Although it may seem counterintuitive that AR serves as a good target in TNBC even though its presence portends a better overall prognosis, the same is true with ER in breast cancer. The presence of these receptors is indicative of a more well-differentiated tumor as both receptors are expressed in normal breast epithelium. However, despite it being a good prognostic indicator, ER serves as a good therapeutic target because the majority of ER^+ tumors are dependent on estrogen and ER. Our data, as well as accumulating preclinical and clinical evidence, suggest that as many as half of TNBC, not just the LAR subtype, may be dependent on AR. Hence, AR may serve as a successful target in such tumors. Furthermore, as the LAR subtype has the second lowest pathologic complete response to chemotherapy, this TNBC subtype is particularly in need of a targeted therapy. Furthermore, our data indicate that even with non-LAR TNBC, that have relatively low amounts of AR and few cells positive, AR increases in suspension culture and supports survival under anchorage-independent conditions. This increase in AR and upregulation of certain AR-regulated proteins under anchorage-independent conditions would not be reflected in TCGA data from primary breast tumors, but was reported at the transcript level in TNBC PDX by Lawson

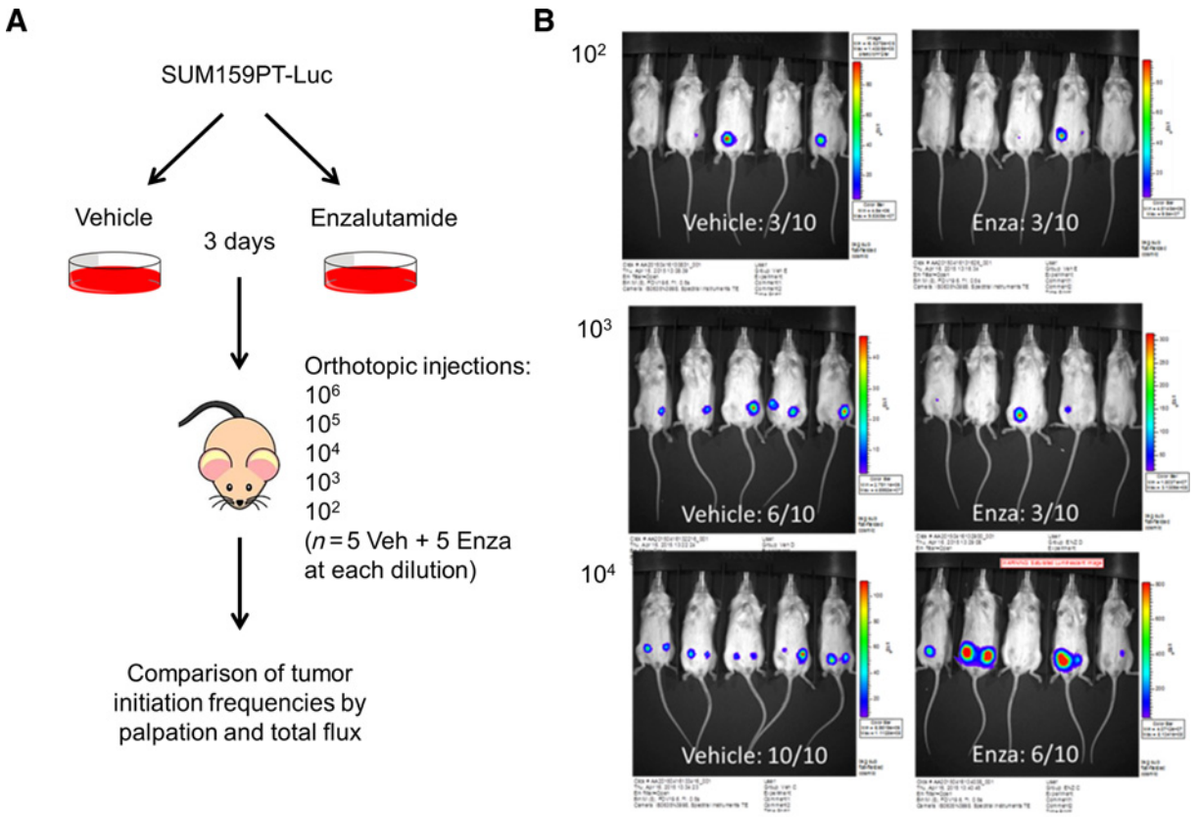

Palpable

Cell #	Vehicle	Enza
1,000,000	10/10	10/10
100,000	10/10	10/10
10,000	10/10	10/10
1,000	7/10	4/10
100	6/10	3/10

P	Veh Stem cell frequency	Enza Stem cell frequency
0.0413	1/463	1/1,221

Total flux

Cell #	Vehicle	Enza
1,000,000	10/10	10/10
100,000	10/10	10/10
10,000	9/10	7/10
1,000	5/10	3/10
100	2/10	1/10

P	Veh Stem cell frequency	Enza Stem cell frequency
0.0478	1/2,401	1/5,907

Figure 6.
Tumor initiation frequency of SUM159PT cells pretreated with enzalutamide. **A,** Schematic of experimental design. **B,** Tumor initiation frequency. Top, luciferase activity, measured as total flux, in mice injected with 10^2–10^4 cells pretreated for 3 days with vehicle control (Veh) or Enza. Bottom, summary of the number of mice per group with tumors as determined by palpation (left) and luciferase activity/total flux (right).

and colleagues (27). Only future profiling and staining of TNBC circulating tumor cells will validate this finding. It will also be interesting to determine whether the GR can subtitute for AR to promote the antiapoptotic effect during metastasis in AR-negative TNBC or whether GR will increase under the selective pressure of long-term antiandrogens as it does in prostate cancer (36, 37). We did not observe GR to increase under anchorage-independent conditions in short term culture (Fig. 2B); however, we are now examining GR in both chronically treated cell lines and patient biopsies from the initial trial of Enza in ER^+ breast cancer.

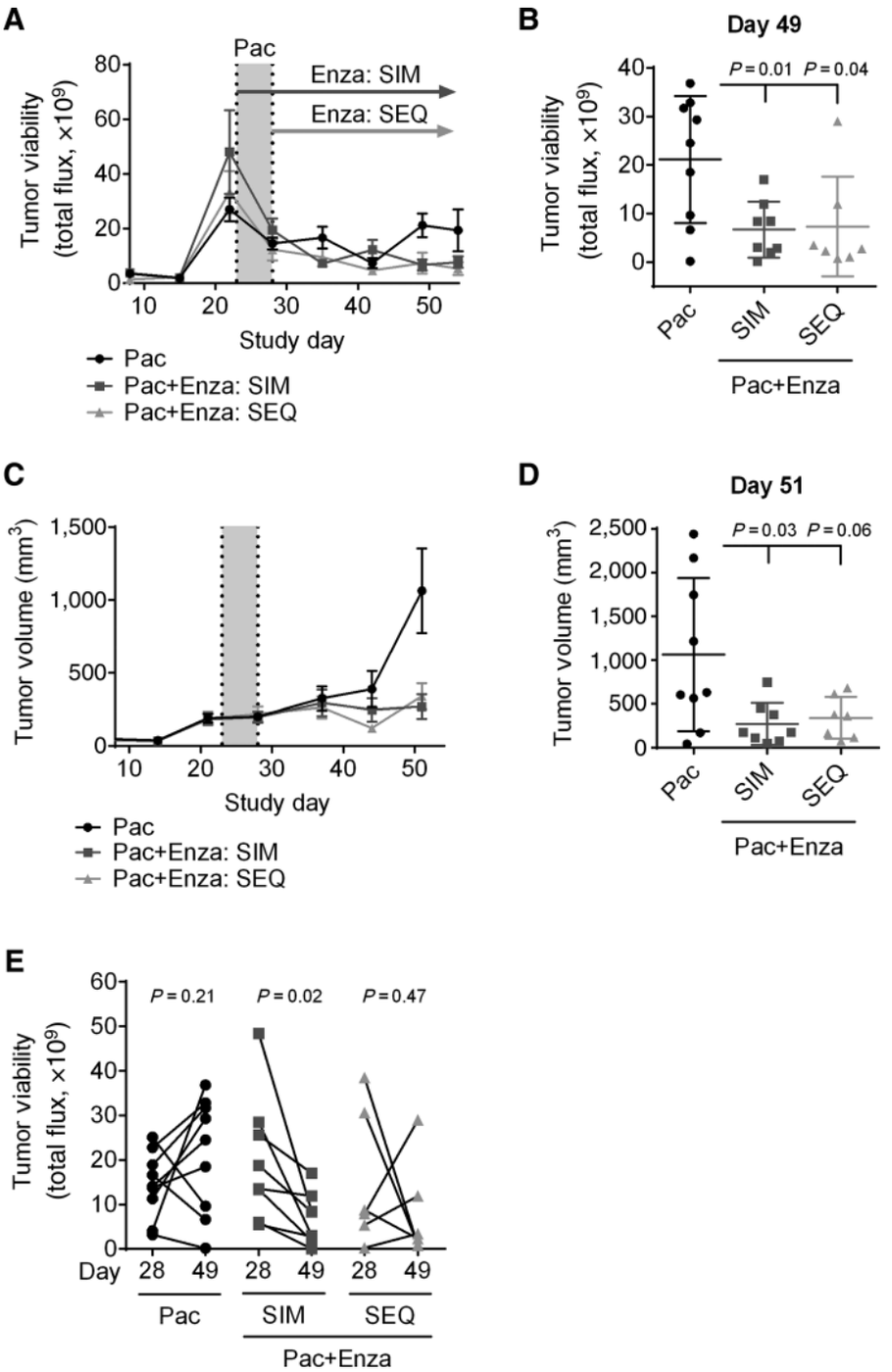

Figure 7.
Enzalutamide and paclitaxel combination therapy is more effective than paclitaxel alone. SUM159PT-TGL cells were bilaterally injected into the fourth mammary fat pads of female, athymic nu/nu mice. Once tumors were established, mice were randomized and matched into three groups. Mice were administered 10 mg/kg/d Pac for five days. Group 1 started Enza simultaneously with Pac (SIM), while group 2 started Enza subsequent to Pac (SEQ). **A,** Tumor cell luciferase activity as measured by total flux over time. **B,** Comparison of total flux on study day 49. **C,** Tumor volume over time. **D,** Comparison of tumor volume on study day 51. **E,** Total flux per mouse between the final day of Pac treatment (day 28) and day 49. Mean ± SD.

Targeting the AR^+, slower growing, anchorage-independent tumor-initiating cells with an antiandrogen, along with chemotherapy to target the proliferative bulk of the tumor, will hopefully prevent recurrant disease and is now being tested in the clinic. The first clinical trial with Enza (NCT01889238) showed clinical benefit when given to women with metastatic disease where the majority of patients had already received chemotherapy (16). The next logical trials with an antiandrogen in AR^+ TNBC are likely to involve chemotherapy with or without antiandrogen in metastatic and then nonmetastatic disease.

Disclosure of Potential Conflicts of Interest

No potential conflicts of interest were disclosed.

Authors' Contributions

Conception and design: V.N. Barton, N.C. D'Amato, A. Elias, J.K. Richer
Development of methodology: V.N. Barton, J.L. Christenson, L.I. Greene, N.S. Spoelstra
Acquisition of data (provided animals, acquired and managed patients, provided facilities, etc.): V.N. Barton, J.L. Christenson, L.I. Greene, K. Butterfield, B. Babbs, N.S. Spoelstra, J.K. Richer
Analysis and interpretation of data (e.g., statistical analysis, biostatistics, computational analysis): V.N. Barton, J.L. Christenson, M.A. Gordon, L.I. Greene, T.J. Rogers, K. Butterfield, N.S. Spoelstra, N.C. D'Amato, A. Elias, J.K. Richer
Writing, review, and/or revision of the manuscript: V.N. Barton, J.L. Christenson, M.A. Gordon, T.J. Rogers, K. Butterfield, N.S. Spoelstra, N.C. D'Amato, A. Elias
Administrative, technical, or material support (i.e., reporting or organizing data, constructing databases): K. Butterfield, J.K. Richer
Study supervision: J.K. Richer

Acknowledgments

The authors acknowledge the Genomics and Microarray Core, the Tissue Culture Core, the Flow Cytometry Shared Resource, and other shared resources of Colorado's NIH/NCI Cancer Center Support Grant P30CA046934.

Grant Support

DOD BCRP Clinical Translational Award BC120183 W81XWH-13-1-0090 to J.K. Richer and A. Elias, R01 CA187733-01A1 to J.K. Richer, and NIH NCI NRSA F31 CA192807-02 to V.N. Barton.

The costs of publication of this article were defrayed in part by the payment of page charges. This article must therefore be hereby marked *advertisement* in accordance with 18 U.S.C. Section 1734 solely to indicate this fact.

Received November 28, 2016; revised March 17, 2017; accepted May 10, 2017; published OnlineFirst May 16, 2017.

References

1. Dent R, Trudeau M, Pritchard KI, Hanna WM, Kahn HK, Sawka CA, et al. Triple-negative breast cancer: clinical features and patterns of recurrence. Clin Cancer Res 2007;13:4429–34.
2. Liedtke C, Mazouni C, Hess KR, Andre F, Tordai A, Mejia JA, et al. Response to neoadjuvant therapy and long-term survival in patients with triple-negative breast cancer. J Clin Oncol 2008;26:1275–81.
3. Kabos P, Haughian JM, Wang X, Dye WW, Finlayson C, Elias A, et al. Cytokeratin 5 positive cells represent a steroid receptor negative and therapy resistant subpopulation in luminal breast cancers. Breast Cancer Res Treat 2011;128:45–55.
4. Al-Hajj M, Wicha MS, Benito-Hernandez A, Morrison SJ, Clarke MF. Prospective identification of tumorigenic breast cancer cells. Proc Natl Acad Sci U S A 2003;100:3983–88.
5. Li X, Lewis MT, Huang J, Gutierrez C, Osborne CK, Wu MF, et al. Intrinsic resistance of tumorigenic breast cancer cells to chemotherapy. J Natl Cancer Inst 2008;100:672–79.
6. Bhola NE, Balko JM, Dugger TC, Kuba MG, Sanchez V, Sanders M, et al. TGF-beta inhibition enhances chemotherapy action against triple-negative breast cancer. J Clin Invest 2013;123:1348–58.
7. Barton VN, D'Amato NC, Gordon MA, Lind HT, Spoelstra NS, Babbs BL, et al. Multiple molecular subtypes of triple-negative breast cancer critically rely on androgen receptor and respond to enzalutamide *in vivo*. Mol Cancer Ther 2015;14:769–78.
8. Micello D, Marando A, Sahnane N, Riva C, Capella C, Sessa F. Androgen receptor is frequently expressed in HER2-positive, ER/PR-negative breast cancers. Virchows Arch 2010;457:467–76.
9. Collins LC, Cole KS, Marotti JD, Hu R, Schnitt SJ, Tamimi RM. Androgen receptor expression in breast cancer in relation to molecular phenotype: results from the Nurses' Health Study. Mod Pathol 2011;24:924–31.
10. Mrklic I, Pogorelic Z, Capkun V, Tomic S. Expression of androgen receptors in triple negative breast carcinomas. Acta Histochem 2013;115:344–48.
11. Safarpour D, Pakneshan S, Tavassoli FA. Androgen receptor (AR) expression in 400 breast carcinomas: is routine AR assessment justified? Am J Cancer Res 2014;4:353–68.
12. Thike AA, Yong-Zheng Chong L, Cheok PY, Li HH, Wai-Cheong Yip G, Huat Bay B, et al. Loss of androgen receptor expression predicts early recurrence in triple-negative and basal-like breast cancer. Mod Pathol 2014;27:352–60.
13. Qi JP, Yang YL, Zhu H, Wang J, Jia Y, Liu N, et al. Expression of the androgen receptor and its correlation with molecular subtypes in 980 chinese breast cancer patients. Breast Cancer 2012;6:1–8.
14. Gucalp A, Tolaney S, Isakoff SJ, Ingle JN, Liu MC, Carey LA, et al. Phase II trial of bicalutamide in patients with androgen receptor-positive, estrogen receptor-negative metastatic Breast Cancer. Clin Cancer Res 2013;19:5505–12.
15. Traina T. Stage I results from MDV3100–11: A 2 stage study of enzalutamide (Enza), an androgen receptor (AR) inhibitor, in advanced AR^+ triple-negative breast cancer (TNBC). Ann Oncol 2015;26:6–9.
16. Traina TA, Miller K, Yardley DA, O'Shaughnessy J, Cortes J, Awarda A, et al. Results from a phase 2 study of enzalutamide (ENZA), an androgen receptor (AR) inhibitor, in advanced AR^+ triple-negative breast cancer (TNBC). J Clin Oncol 2015;33:1003.
17. Horwitz KB, Dye WW, Harrell JC, Kabos P, Sartorius CA. Rare steroid receptor-negative basal-like tumorigenic cells in luminal subtype human breast cancer xenografts. Proc Natl Acad Sci U S A 2008;105:5774–79.
18. Graham JD, Mote PA, Salagame U, van Dijk JH, Balleine RL, Huschtscha LI, et al. DNA replication licensing and progenitor numbers are increased by progesterone in normal human breast. Endocrinology 2009;150:3318–26.
19. Asselin-Labat ML, Vaillant F, Sheridan JM, Pal B, Wu D, Simpson ER, et al. Control of mammary stem cell function by steroid hormone signalling. Nature 2010;465:798–802.
20. Beato M, Herrlich P, Schutz G. Steroid hormone receptors: many actors in search of a plot. Cell 1995;83:851–57.
21. Cloke B, Huhtinen K, Fusi L, Kajihara T, Yliheikkila M, Ho KK, et al. The androgen and progesterone receptors regulate distinct gene networks and cellular functions in decidualizing endometrium. Endocrinology 2008;149:4462–74.
22. Robinson JL, Macarthur S, Ross-Innes CS, Tilley WD, Neal DE, Mills IG, et al. Androgen receptor driven transcription in molecular apocrine breast cancer is mediated by FoxA1. EMBO J 2011;30:3019–27.
23. Wang Q, Li W, Zhang Y, Yuan X, Xu K, Yu J, et al. Androgen receptor regulates a distinct transcription program in androgen-independent prostate cancer. Cell 2009;138:245–56.
24. Yu J, Yu J, Mani RS, Cao Q, Brenner CJ, Cao X, et al. An integrated network of androgen receptor, polycomb, and TMPRSS2-ERG gene fusions in prostate cancer progression. Cancer Cell 2010;17:443–54.
25. Cimino-Mathews A, Hicks JL, Illei PB, Halushka MK, Fetting JH, De Marzo AM, et al. Androgen receptor expression is usually maintained in initial surgically resected breast cancer metastases but is often lost in end-stage metastases found at autopsy. Hum Pathol 2012;43:1003–11.
26. McNamara KM, Moore NL, Hickey TE, Sasano H, Tilley WD. Complexities of androgen receptor signalling in breast cancer. Endocr Relat Cancer 2014;21:161–81.
27. Lawson DA, Bhakta NR, Kessenbrock K, Prummel KD, Yu Y, Takai K, et al. Single-cell analysis reveals a stem-cell program in human metastatic breast cancer cells. Nature 2015;526:131–35.
28. Feng J, Li L, Zhang N, Liu J, Zhang L, Gao H, et al. Androgen and AR contribute to breast cancer development and metastasis: an insight of mechanisms. Oncogene 2016;35:1–16.
29. Christenson JL, Butterfield KT, Spoelstra NS, Norris JD, Josan JS, Pollock JA, et al. MMTV-PyMT and derived Met-1 mouse mammary tumor cells as models for studying the role of the androgen receptor in triple-negative breast cancer progression. Horm Cancer 2017;8:69–77.
30. Doane AS, Danso M, Lal P, Donaton M, Zhang L, Hudis C, Gerald WL. An estrogen receptor-negative breast cancer subset characterized by a hormonally regulated transcriptional program and response to androgen. Oncogene 2006;25:3994–4008.

31. Farmer P, Bonnefoi H, Becette V, Tubiana-Hulin M, Fumoleau P, Larsimont D, et al. Identification of molecular apocrine breast tumours by microarray analysis. Oncogene 2005;24:4660–71.
32. Lehmann BD, Bauer JA, Chen X, Sanders ME, Chakravarthy AB, Shyr Y, Pietenpol JA. Identification of human triple-negative breast cancer subtypes and preclinical models for selection of targeted therapies. J Clin Invest 2011;121:2750–67.
33. Booth BW, Boulanger CA, Anderson LH, Jimenez-Rojo L, Brisken C, Smith GH. Amphiregulin mediates self-renewal in an immortal mammary epithelial cell line with stem cell characteristics. Exp Cell Res 2010;316:422–32.
34. Marotta LL, Almendro V, Marusyk A, Shipitsin M, Schemme J, Walker SR, et al. The JAK2/STAT3 signaling pathway is required for growth of CD44(+)CD24(-) stem cell-like breast cancer cells in human tumors. J Clin Invest 2011;121:2723–35.
35. Masuda H, Baggerly KA, Wang Y, Zhang Y, Gonzalez-Angulo AM, Meric-Bernstam F, et al. Differential response to neoadjuvant chemotherapy among 7 triple-negative breast cancer molecular subtypes. Clin Cancer Res 2013;19:5533–40.
36. Arora VK, Schenkein E, Murali R, Subudhi SK, Wongvipat J, Balbas MD, et al. Glucocorticoid receptor confers resistance to antiandrogens by bypassing androgen receptor blockade. Cell 2013;155:1309–22.
37. Isikbay M, Otto K, Kregel S, Kach J, Cai Y, Vander Griend DJ, et al. Glucocorticoid receptor activity contributes to resistance to androgen-targeted therapy in prostate cancer. Horm Cancer 2014;5:72–89.